Acta Tropica 206 (2020) 105444

Contents lists available at ScienceDirect

Acta Tropica

journal homepage: www.elsevier.com/locate/actatropica

Evaluation of NanoLuc, RedLuc and Luc2 as bioluminescent reporters in a cutaneous leishmaniasis model

Victor S. Agostino[a], Cristiana M. Trinconi[a], Mariana K. Galuppo[a], Helen Price[b], Silvia R.B. Uliana[a,*]

[a] Department of Parasitology, Biomedical Sciences Institute, University of Sao Paulo, Sao Paulo CEP 05508-000, Brazil
[b] Centre for Applied Entomology and Parasitology, School of Life Sciences, Keele University, Newcastle-under-Lyme, Staffordshire ST5 5BG, United Kingdom

ARTICLE INFO

Keywords:
Leishmania
Drug screening
Bioluminescent reporters
Bioimaging
NanoLuc
Red-shifted luciferase

ABSTRACT

New drugs for the treatment of human leishmaniasis are urgently needed, considering the limitations of current available options. However, pre-clinical evaluation of drug candidates for leishmaniasis is challenging. The use of luciferase-expressing parasites for parasite load detection is a potentially powerful tool to accelerate the drug discovery process. We have previously described the use of *Leishmania amazonensis* mutants expressing firefly luciferase (Luc2) for drug testing. Here, we describe three new mutant *L. amazonensis* lines that express different variants of luciferases: NanoLuc, NanoLuc-PEST and RedLuc. These mutants were evaluated in drug screening protocols. NanoLuc-parasites, in spite of high bioluminescence intensity *in vitro*, were shown to be inadequate in discriminating between live and dead parasites. Bioluminescence detection from intracellular amastigotes expressing NanoLuc-PEST, RedLuc or Luc2 proved more reliable than microscopy to determine parasite killing. Increased sensitivity was observed *in vivo* with RedLuc-expressing parasites as compared to NanoLuc-expressing *L. amazonensis*. Our data indicates that NanoLuc is not suitable for *in vivo* parasite burden determination. Additionally, RedLuc and the conventional luciferase Luc2 demonstrated equivalent sensitivity in an *in vivo* model of cutaneous leishmaniasis.

1. Introduction

The leishmaniases are a complex group of devastating diseases with a wide clinical spectrum varying from self-healing tegumentary to fatal visceral forms. Over 20 species of *Leishmania spp*. are pathogenic to humans leading to variable clinical manifestations depending on the parasite species and host immunological response. Within the tegumentary form, the disease can be further classified in cutaneous, mucocutaneous, diffuse and disseminated leishmaniasis (Burza et al., 2018). *Leishmania (Leishmania) amazonensis* is one of the most prevalent agents of human cutaneous leishmaniasis (CL) in the Amazon region of Brazil. It is also the main etiological agent of diffuse cutaneous leishmaniasis (DCL) in South America (Convit et al., 1993), a rare and aggressive form of disease characterized by the appearance of multiple non-tender and non-ulcerating papules or nodules widespread in the body. DCL is a chronic disease and is considered refractory to the current available anti-*Leishmania* therapeutic arsenal (Zerpa et al., 2007).

The parasite can be transmitted by several species of female hematophagous sandflies, most of them within the genus *Phlebotomus*, in the Old World, and *Lutzomyia*, in the New World (Akhoundi et al., 2016). Leishmaniases are distributed worldwide and endemic in over 90 countries or territories. According to the World Health Organization, the annual incidence of the disease is approximately 1 million new cases (Bern et al., 2012; WHO, 2015).

The treatment of leishmaniases is limited to a few drugs and most of them have been in use for a long time without significant upgrading (Uliana et al., 2017). The therapeutic arsenal currently available includes pentavalent antimonials, amphotericin B, pentamidine, miltefosine and paromomycin. Miltefosine is the only drug which is administered orally (Sundar and Olliaro, 2007), whereas all the others must necessarily be administered parenterally. All those drugs may induce serious side effects, ranging from nephro-hepatotoxicity to teratogenicity (Sundar and Singh, 2018). The toxicity is even more pronounced in malnourished patients, a common occurrence with advanced visceral leishmaniasis. Moreover, loss of efficacy of pentavalent antimonials and miltefosine has been reported (Ponte-Sucre et al., 2017). Thus, the identification of new drugs for leishmaniasis treatment with better efficacy and safety profiles is an urgent issue.

Preclinical drug development against leishmaniasis includes *in vitro*

* Corresponding author.
E-mail address: srbulian@icb.usp.br (S.R.B. Uliana).

https://doi.org/10.1016/j.actatropica.2020.105444
Received 6 January 2020; Received in revised form 11 March 2020; Accepted 11 March 2020
Available online 13 March 2020

and *in vivo* tests. *In vitro* tests are preferably performed against the intracellular amastigote stage and *in vivo* tests employ animal models, mostly mice and hamsters. The use of reporter proteins detectable in intact animals represented a great advance for the challenging demonstration of drug efficacy of antileishmanial compounds in experimental models of the disease (Calvo-Alvarez et al., 2018; Jaiswal et al., 2016; Rocha et al., 2013). Furthermore, the strategy addresses the important ethical aspects of reducing the number of animals needed for each experiment as well as refining the handling and information derived from each animal (two out of the 3Rs advocated for ethical preclinical research. We have previously employed mutant parasite lines expressing a modified firefly luciferase as an experimental tool for testing candidate compounds *in vitro* and *in vivo* (Reimão et al., 2015, 2013; Trinconi et al., 2016).

Luciferases are a class of enzymes commonly found in nature in fireflies and in several marine organisms, such as jellyfish or copepods, that generates light in the presence of a specific substrate (Avci et al., 2018; Yan et al., 2019). Natural luciferases have been genetically modified to improve their specific activity, through increased intensity of light production, and/or altered wavelength to improve detection. Amongst many modified luciferases already produced, three of these were chosen for the analysis described here: RedLuc (RL), NanoLuc (NL) and its variation NanoLuc-PEST (NLP). NL and NLP were derived from Oluc, a luciferase isolated from the deep-sea shrimp (*Oplophorus gracilirostris*) (Hall et al., 2012). NL was shown to achieve greater efficiency than the parent protein in the presence of furimazine, its appropriate substrate, modified from coelenterazine (Hall et al., 2012). Furthermore, NL's intracellular half-life of 6 h leads to intracellular accumulation of the enzyme, which also potentiates light emission. NLP was obtained by inserting a PEST motif (García-Alai et al., 2006; Rechsteiner and Rogers, 1996) into the C-terminus region of the protein, resulting in a shorter intracellular half-life of about 20 min. RedLuc, a red-shifted luciferase, is a firefly (*Luciola cruciata*) luciferase gene modified by the substitution of an isoleucine by a valine in the position 48 (p.I48V), which modifies the substrate (luciferin) cleavage, resulting in the production of light with a wavelength above 600 nm (Branchini et al., 2005a). Long wavelength light can penetrate more easily in tissue barriers, which could potentially enhance the sensitivity detection of lower parasite burdens.

Here, we described the application of these modified luciferases (NL, NLP and RL) *in vitro* and in an *in vivo* model of cutaneous leishmaniasis.

2. Materials and methods

2.1. Parasites

Wild-type *Leishmania amazonensis* (MHOM/BR/1973/M2269) was cultivated at 25 °C in 199 culture medium (Sigma-Aldrich, St. Louis, MO, USA), complemented with HEPES 40 mM, pH 7.4, adenine 0.1 mM, hemin 0.005% and supplemented with heat-inactivated bovine foetal serum 10% (Gibco®), and penicillin/streptomycin 100 μg/ml. A mutant line of *L. amazonensis* expressing Luc2, obtained as described (Reimão et al., 2015), was grown in media supplemented with 32 μg/ml hygromycin. Mutant lines obtained in this work were cultivated in media containing 32 μg/ml G418. Parasites were subcultured weekly.

2.2. Generation of L. amazonensis line expressing the modified luciferases

NL, NLP and RL constructs were obtained by cloning NanoLuc (616 bb), NanoLuc-PEST (639 bp) and RedLuc (1647 bp) ORFs into the pSSU-Neo plasmid, which contains complementary sequences to the *Leishmania* small subunit ribosomal DNA and a neomycin resistance encoding gene (Berry et al., 2018). Upon transfection, the linearized plasmid was expected to integrate into the parasite genome.

Promastigotes were transfected as previously described by Coburn et al. (1991) using 5 μg of linearized insert. After 24 h, the selection drug (G418) was added to a concentration of 32 μg/ml. Cultures were plated on semi-solid M199 medium supplemented with 1.2 μg/mL biopterin, 1% agar, 2% urine and 32 μg/mL G418 for clone selection. Isolated clones were randomly selected and expanded. Integration into the SSU rDNA was confirmed through PCR amplification with primers complementary to sequences inside and outside the transfected cassette. Primers S1 (5′-GATCTGGTTGATTCTGCCAG-3′) and S4 (5′-GATCCAGCTGCAGGTTCACC-3′) anneal to the SSU rDNA sequence (Uliana et al., 1991) flanking the insertion sites, and primers NanoLuc-REV (5′ TACCAGTGTGCCATAGTGCA 3′), RedLuc-REV (5′ ACGATGGTCTTGATGGTGGT 3′) and Neo-FOR (5′ TATCGCCTTCTTG ACGAGTTCT 3′) are complementary to the cassette.

2.3. Bioluminescence detection assay

Logarithmic phase promastigotes were washed and suspended in PBS to a final density of 10^6 promastigotes/mL. Parasites were serially diluted in final volumes of 100 μL and incubated in lysis buffer containing either furimazine (NanoGlo Assay System, Promega), for mutants expressing NL and NLP, or luciferin (One-Glo luciferase Assay System, Promega), for mutants expressing RL and Luc2. Furimazine was added to the lysis buffer in a 1:200 ratio and luciferin was added in a 1:5 ratio. Bioluminescence was measured using a PolarStar Omega luminometer (BMGLabTech).

2.4. Susceptibility assays of intracellular amastigotes

Bone marrow-derived macrophages (BMDM) were obtained as described (Reimão et al., 2015) and plated in white 96-well plates (8×10^4 cells/well) or in 24-well plates (3×10^5 cells/well) with round glass coverslips applied to the bottom of the wells. After incubation for 24 h at 37 °C in a 5% CO_2 atmosphere, cells were infected with stationary phase promastigotes (fourth day of culture) in a proportion of 20 parasites: 1 macrophage. After 4 h incubation at 34 °C, cultures were washed to remove the remaining free promastigotes. Fresh medium containing several concentrations of miltefosine (Sigma-Aldrich), varying from 1 to 30 μM, was added and the plates were incubated for 96 h at 34 °C. The supernatant was discarded, and luciferase substrates were added to the 96-well plate as described in the Section 2.3. After homogenization, light production was detected in a PolarStar Omega luminometer (BMGLabTech). Parasite survival in treated samples was determined based on the ratio of treated/untreated cells. Macrophages cultivated in round coverslips were fixed with 50% methanol in PBS and stained with the Romanowsky type Instant Prov kit (Newprov, Pinhais, PR, Brazil). The ratio of infected cells was calculated by counting 100 macrophages per replicate. Half maximal inhibitory concentration (IC_{50}) was determined from bioluminescence and microscopy assays by sigmoidal regression of the dose-response curves using GraphPad Prism 8 software (CA, USA). Experiments were performed in triplicate and repeated at least three times.

2.5. Mice infection and parasite quantification

Animal experiments were approved by the Ethics Committee for Animal Experimentation (Protocol 178/2012) in agreement with the guidelines of the Sociedade Brasileira de Ciência de Animais de Laboratório (SBCAL) and of the Conselho Nacional de Controle da Experimentação Animal (CONCEA).

Female BALB/c mice (30 to 60 days-old) were inoculated subcutaneously with 10^6 stationary-phase promastigotes of La-NL, La-RL or La-Luc2 in the left hind footpad. Lesion development was followed up weekly. Retrieval and purification of amastigotes from lesions was done as described previously (Uliana et al., 1999). Quantification of amastigotes recovered from lesions was performed by limiting dilution (Lima et al., 1997). Determination of parasite burden was calculated

using the formula LDAU = GM x RF (Calvo-Álvarez et al., 2015), in which LDAU is the parasite burden indicated in limiting dilution assay units, GM is the geometric mean of titer from the replicates and RF is the reciprocal fraction of the homogenized lesion added to the first well. In this formula, titter is the last dilution where live parasites were observed.

Bioluminescence quantification in live animals was performed as described (Reimão et al., 2013). Imaging was performed after intraperitoneal administration of 75 mg/kg luciferin (VivoGlo™, Promega) or 1:40 diluted furimazine (NanoGlo™, Promega) in sterile PBS and in 100 µl final volume. Animals were anesthetized under a 2.5% isoflurane atmosphere and transferred to the imaging chamber, where they were kept in a 1.5% isoflurane atmosphere during imaging. Images were acquired 15 min after substrate administration using an IVIS Spectrum (Caliper Life Sciences) with 2 min exposure time. Bioluminescence readings for the whole animal were obtained. A region of interest (ROI) was defined as a region encompassing an infected footpad. The same ROI (shape and size) was used to quantify measured light units in all animals studied. Average radiance (photons/second/square centimetre/steradian) was quantified by Living Image 4.3.1 (Caliper Life Sciences), representing total photon emission from a ROI. A bioluminescence background was initially obtained using the same ROI in an uninfected mouse. Alternatively, background was measured using the ROI positioned at the contralateral uninfected footpad. The background value was subtracted from all infected footpad readings. Pseudocolor imaging was generated based on the photon signal to represent light intensity from the infected footpads, ranging from red to blue meaning the most to the least intense.

For immediate quantification of light production by parasites inoculated in mice tissues, 10^5 stationary-phase promastigotes or amastigotes purified from lesions were inoculated in the left hind footpad and animals were imaged one-hour post-injection.

Parasite burden of infected mice was also evaluated by *ex vivo* bioluminescence. For these assays, the material recovered from lesions was suspended in 2 mL PBS and 20 µL from the total amastigote extract of each infected animal was incubated in the presence of the respective substrate and submitted to bioluminescence quantification, as described above.

2.6. Statistical analysis

All statistical analyses were performed by GraphPad Prism 8 (CA, USA), using ANOVA *one-way* test and multiple comparisons Dunnett's test. *P* values $\leqslant 0.05$ were considered statistically significant.

3. Results and discussion

3.1. Generation and phenotypic characterization of L. amazonensis mutants expressing NanoLuc (NL), NanoLuc-PEST (NLP) and RedLuc (RL)

Constructs containing the modified luciferase genes were double digested with endonucleases *Pac*I and *Pme*I, to linearize the cassette. Purified inserts (Fig. 1A) were transfected into wild-type (WT) *L. amazonensis* to generate mutants expressing NL (La-NL), NLP (La-NLP) and RL (La-RL). Integration into the small subunit rDNA (SSU) gene was assessed by PCR (Fig. 1B). Primers for SSU sequences upstream and downstream to the expected integration region were designed and paired with primers corresponding to the luciferase gene or drug resistance marker (Fig. 1A). PCR products with the expected sizes confirmed the integration of the linearized DNA fragment in the expected *locus* (Fig. 1B). Clones were obtained and their growth curves were characterized. The growth of these transfected parasites was indistinguishable from the WT parasites (Fig. 1C), indicating that the integration of the cassette into the parasite genome did not impair cell growth.

The infectivity of *L. amazonensis* mutant lines *in vitro* was tested using BMDM. Cells were infected with stationary-phase promastigotes and maintained in culture for 48 h. The percentage of infected macrophages and the number of amastigotes per macrophage were determined by optical microscopy and compared to infections with the WT parasite (Table 1). No significant differences were observed among the different mutant lines.

The infectivity *in vivo* of each mutant line was evaluated in the BALB/c mice model. Lesion development in mice infected with the mutant lines was delayed when compared to WT parasites (Supplementary Material Fig. S1). This reduced virulence could be related to the number of *in vitro* parasite sub-cultures (Magalhães et al., 2014); however, repeated infections in mice did not accelerate lesion development. Although the La-Luc2 line, previously obtained by the same method, maintained its infectivity profile, the possibility of impairment of the *in vivo* fitness of luciferase mutant parasites by the expression of those particular proteins cannot be excluded at present. Other studies in *L. infantum* expressing red-shifted luciferases have been done and did not report infectivity changes (Álvarez-Velilla et al., 2019; Eberhardt et al., 2019).

3.2. Biouminescence of promastigotes expressing NL, NLP and RL

Luciferase activity of mutant lines was evaluated by analysing light production of serially diluted promastigotes incubated in the presence of their respective substrates (Fig. 2A). Promastigotes expressing the conventional luciferase Luc2 (Trinconi et al., 2018) were also evaluated and used as a reference. Light emission, expressed in relative bioluminescence units (RLU), was linearly correlated with the number of parasites ($r^2 > 0.9894$). NL-expressing parasites were the brightest with light output up to 1000-fold higher than NLP and over 100-fold higher than RL and Luc2 (Fig. 2). NLP produced the narrowest range of light intensity output throughout the curve. The sensitivity for detecting RL-expressing parasites was higher than Luc2 when 100 or less parasites were assayed. The curve profiles for RL and Luc2 promastigotes overlapped when more than 1000 parasites were evaluated. The detection limits for light production by NL, NLP and RL were 1, 10 and 10 parasites, respectively, while 100 parasites were necessary to detect Luc2 bioluminescence.

Light output from these parasites increased over the course of 60 min after substrate addition, but maintained the bioluminescence curve profiles (Supplementary Material Fig. S2).

La-NL and La-NLP light emission patterns were in agreement with findings described by Hall et al. (2012), who developed NL and its derivatives through enzyme optimization and coelenterazine modification. An intracellular half-life of at least 6 h for the NL protein, as opposed to 3 h for Luc2 (Thorne et al., 2010), leads to NL accumulation in eukaryotic cells and, in theory, to a greater light production. In fact, NL half-life in *L. mexicana* mutant lines was demonstrated to be greater than 8 h (Berry et al., 2018). Therefore, NL demonstrated better *in vitro* performance in comparison to all the other luciferases tested with a light emission 100 to 1000 times more intense, including the conventional luciferase, Luc2.

On the other hand, NL slow kinetics of decay made it too stable to be used in promastigote viability assays, which was also seen in NL-expressing *L. mexicana* parasites (Berry et al., 2018). For example, in conventional 24-hour assays using increasing concentrations of amphotericin B against promastigotes expressing NL, it was not possible to detect the expected decline in light intensity in treated parasites (Supplementary Material Figure S3). For that reason, further *in vitro* experiments were performed using NLP, RL and Luc2, whereas NL was saved for *in vivo* testing.

3.3. Drug susceptibility testing in intracellular amastigotes

To test these mutant lines in drug susceptibility assays, macrophages infected with La-NLP, La-RL and La-Luc2 were treated with

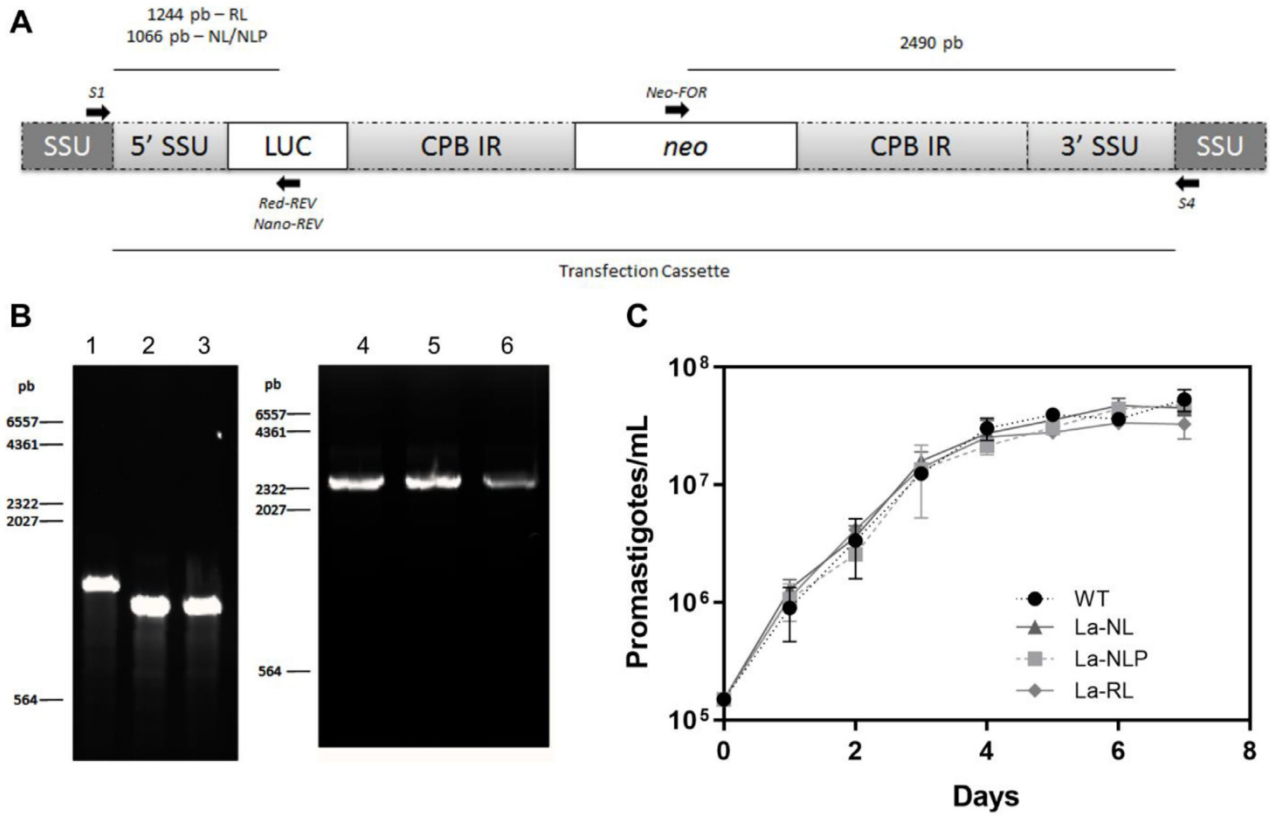

Fig. 1. Generation of *L. amazonensis* transgenic lines expressing modified luciferases. (**A**) Schematic representation of the linear cassette integrated into the SSU rDNA *locus*. SSU: small subunit rDNA; 5′/3′ SSU: SSU homologous regions included in the cassette; LUC: coding sequence of modified luciferases; CPB IR: *L. mexicana* cysteine protease B intergenic region; *neo*: neomycin-phosphotransferase gene; arrows: primers used for PCR. (**B**) PCR products from La-RL (lanes 1 and 4), La-NL (lanes 2 and 5) and La-NLP (lanes 3 and 6) genomic DNA with the pairs of primers S1/Red-REV (lane 1), S1/Nano-REV (lanes 2 and 3) and S4/Neo-FOR (lanes 4 to 6). (**C**) Growth curve of transfected and wild-type parasites. Results are the mean and standard deviation of a representative experiment of three independent experiments.

Table 1
Evaluation of BMDM infection by WT and mutant *L. amazonensis* lines expressing modified luciferases.

	Infection (%)	Amastigotes/MØ
La-WT	56.6 ± 4,36	2.8 ± 0.3
La-NL	47.6 ± 4,04	2.0 ± 0.2
La-NLP	44.4 ± 3,78	1.9 ± 0.05
La-RL	43.1 ± 2,46	1.8 ± 0.1

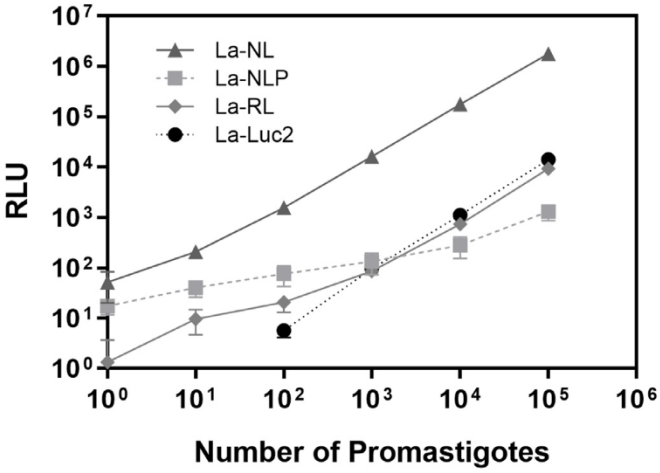

Fig. 2. Luciferase activity in promastigotes of *L. amazonensis* transfected lines. Promastigotes were serially diluted and bioluminescence was measured 10 min after substrate addition. Results are the mean and standard deviation of a representative experiment of three independent experiments. RLU: relative light units.

different concentrations of miltefosine (Fig. 3 and Table 2) and the percentage of infected macrophages was determined after 72 h by standard microscopy or bioluminescence intensity. Miltefosine was chosen given its good activity against *L. amazonensis in vitro* and *in vivo* (Coelho et al., 2014). The calculated IC_{50} values were statistically similar between the mutants for both methods (Table 2). The bioluminescence assay produced robust dose-response curves, consistent in all mutants. All three luciferases – NLP, RL and Luc2 – showed to be equally effective in the assessment of drug susceptibility in intracellular amastigotes (Fig. 3B). The results determined through optical microscopy revealed wider standard deviations and therefore higher variability (Fig. 3A). This can be explained by the method's limitations, such as the examiner's choice of fields to count.

We showed that NLP, RL and Luc2 were equally able to report amastigote viability. Interestingly, light intensity from La-NLP and La-RL in intracellular amastigotes were higher than light emitted by La-Luc2 (Supplementary Material Figure S4) while the opposite was observed for promastigotes (Fig. 2, Supp. Fig. S2). A distinct rate of NLP/RL protein or RNA degradation in amastigotes might explain this observation. The cassettes with NLP and RL genes contain the *L. mexicana* cysteine protease B 2.8 3′ untranslated region (UTR), downstream to the NLP or RL genes. On the other hand, the Luc2 cassette has the tubulin 3′ UTR downstream to the coding sequence. The CPB UTR, originally derived from a stage-regulated gene, may be driving this increased bioluminescence in amastigotes (Mißlitz et al., 2000;

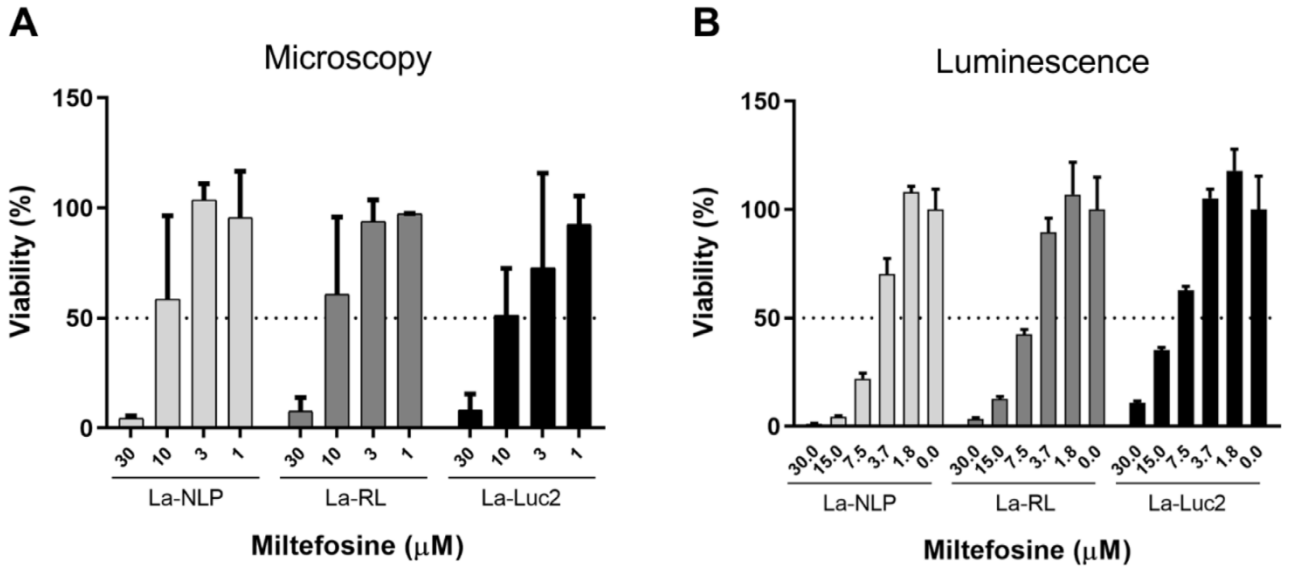

Fig. 3. Comparison of bioluminescence and microscopy for the evaluation of drug susceptibility. Macrophages infected with La-NLP, La-RL and La-Luc2 were treated with increasing concentrations of miltefosine for 72 h. Parasite viability was determined using microscopy **(A)** and bioluminescence-based **(B)** techniques. Viability was calculated in reference to the untreated control, considered as 100% viable, for each line. Data are mean and standard deviation of at least three independent experiments.

Table 2
Miltefosine IC_{50} for intracellular amastigotes calculated by bioluminescence or microscopy.

Lines	Bioluminescence[a]	Microscopy[a]
La-NLP	6.96 ± 0.99	11.85 ± 3.32
La-RL	7.67 ± 1.46	12.4 ± 3.36
La-Luc2	7.71 ± 1.71	8.32 ± 3.43

[a] Results are the average and standard error of the mean (SEM) of at least three independent experiments.

Brooks et al., 2001).

3.4. Comparison of modified luciferases in an in vivo model

In order to compare the *in vivo* bioluminescence of the modified luciferases, mutant lines with higher *in vitro* light emission - La-NL and La-RL - were selected. BALB/c mice were infected with La-NL and La-RL and parasite load was evaluated by bioimaging and limiting dilution once lesions were well established. Parasite burden determined by limiting dilution was at least 10-fold higher in La-NL-infected animals than in La-RL-infected mice (Fig. 4B). Conversely, bioluminescence detected from La-RL infected animals was up to 1000-fold greater than light from La-NL mice (Fig. 4A and B). Amastigotes freshly extracted from lesions were also used to determine *ex vivo* bioluminescence and qualitatively compare the parasite burden between infected animals (Fig. 4C). *In vitro* light emission in the La-NL lesion extracts was higher than in La-RL lesions, confirming the higher parasite burden of La-NL-infected mice detected by limiting dilution. The ratio between the number of amastigotes detected in the limiting dilution assay by the relative light units detected by bioimaging was used as an arbitrary measure of *in vivo* sensitivity (Fig. 4D). The putative number of amastigotes necessary to emit one RLU *in vivo* was 1000-fold greater for La-NL than La-RL.

Light produced by the reaction of RL and its substrate is emitted within a narrow spectrum above 600 nm, as shown by studies with similar luciferases (Branchini et al., 2005b; 2010). NL, on the other hand, produces a narrow spectrum at 450 nm. Results shown here are consistent with the previous understanding that La-RL derived light may overcome tissue barriers more efficiently than light produced by La-NL. Our experiments showed that animals infected with La-RL that developed lesions with approximately 10^6 parasites displayed greater levels of bioluminescence than La-NL lesions bearing about 10^9 amastigotes.

Considering the *in vivo* performance of La-RL, the mutant line was moved forward to be compared with Luc2, the conventional firefly luciferase. La-RL or La-Luc2 infected mice were evaluated nine weeks post infection by bioimaging and limiting dilution (Fig. 5A and B). A slower progression in lesion size was observed in the group infected with La-RL (Fig. 5D). In agreement with that observation, the parasite burden was about 6-fold higher in La-Luc2 infections compared with La-RL-infected mice (Fig. 5B). A bioluminescence pattern congruent with the limiting dilution data was observed (Fig. 5A and B). The *ex vivo* amastigote bioluminescence assay confirmed the difference in parasite burden between groups with a more uniform signal within the group (Fig. 5C) compared to bioimaging and limiting dilution quantifications. The *in vivo* light output was not statistically different between groups.

Aiming to avoid the influence of any differences in lesion development between the La-RL and La-Luc2 lines, mice were bioimaged 1 h after inoculation with a fixed number of parasites. Freshly purified lesion-derived amastigotes or stationary phase-promastigotes were injected at the anterior and posterior footpads. One hour later, bioluminescence was measured. No significant differences were observed between footpads inoculated with amastigotes and promastigotes of the same line. The comparison of light intensity emitted by La-RL and La-Luc2 was also statistically identical, indicating equivalent *in vivo* detection for RL and Luc2 as reporters in a cutaneous leishmaniasis model (Fig. 6).

RL showed to be a promising viability reporter both in *in vitro* and *in vivo* assays. Unexpectedly, RL displayed sensitivity similar to Luc2 in our model, even though its light is emitted in a wavelength above 600 nm. According to Liang et al. (2012), Luc2 produces light in a broad spectrum of emission, from 540 to 640 nm. Although some of this light may be blocked by tissues, as with NL, part of it is emitted over 600 nm and therefore interference would be less important. On the other hand, in a model where skin lesions are being evaluated, less tissue barriers are present. Nevertheless, there is still room to investigate the use of this luciferase in visceral leishmaniasis, where the light emitted by the parasite might encounter more tissue barriers. Our findings lead to the conclusion that, as observed for Luc2, RL was

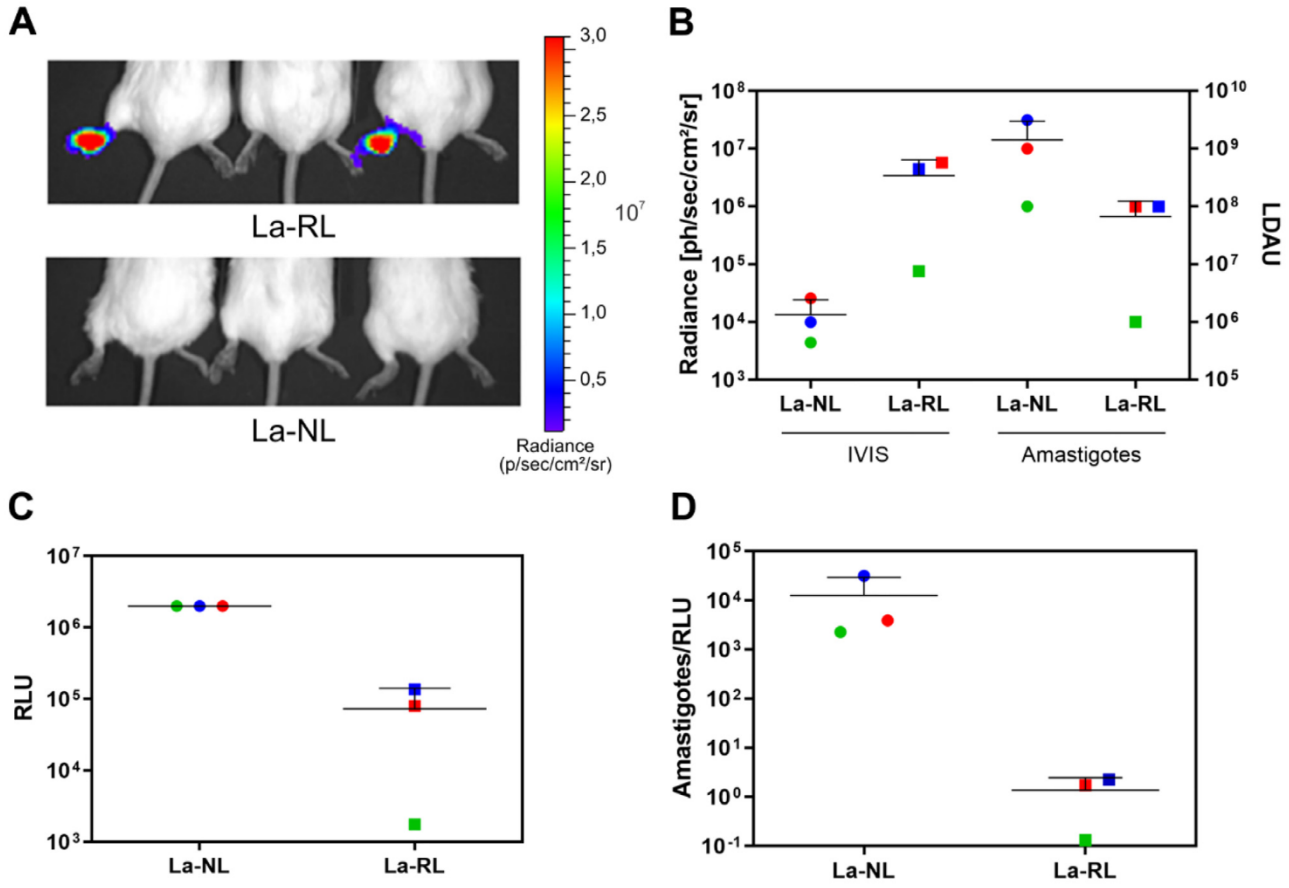

Fig. 4. Comparison of *in vivo* and *ex vivo* bioluminescence emission by La-NL and La-RL-infected mice. BALB/c mice ($n = 3$) were inoculated with 10^6 La-NL or La-RL promastigotes at the left hind footpad. The parasite burden was evaluated at the 31st week post infection by *in vivo* bioluminescence imaging (**A** and **B**), limiting dilution (**B**) and *ex vivo* bioluminescence (**C**). The putative number of amastigotes per RLU captured during bioimaging was calculated as the ratio between amastigotes detected by limiting dilution and relative light units (**D**). IVIS: *in vivo* imaging system; LDAU: limiting dilution assay units, meaning total number of amastigotes in the footpad; RLU: relative light units.

effective for both *in vitro* and *in vivo* viability assays while NLP is a good option for *in vitro* studies.

New strategies for imaging will bring great benefits onto biological preclinical evaluation of drugs and diseases. Interesting avenues are being pursued by improving reporter enzymes as well as the bioluminescence properties of the substrates (Kuchimaru et al., 2016; Iwano et al., 2018), or both (Yeh et al., 2017). For example, a near infrared shift on emission obtained by a modified luciferase substrate resulted in great improvements in sensitivity of detection particularly from deep tissues (Kuchimaru et al., 2016) and even allowing detection of single cells in deep tissues of live animals (Iwano et al., 2018). These tools are beginning to be employed to study the relationship between parasites and their hosts and are opening a whole new set of possibilities (De Niz et al., 2019).

4. Conclusion

Altogether, these findings bring new insights regarding the use of modified luciferases in the drug discovery process for infectious diseases. NL demonstrated strong *in vitro* bioluminescence and higher stability over the other luciferases. However, its application might be somewhat restricted to *in vitro* experiments here unexplored, whereas Luc2 and RL have apparently greater *in vivo* application, even though their light emission *in vitro* is less intense than NL. All luciferases, except for NL, showed to be useful tools in the report of intracellular amastigotes viability. Finally, we have demonstrated that a red-shifted luciferase does not enhance light detection in a cutaneous leishmaniasis model, displaying similar *in vivo* bioluminescent potential in comparison to the conventional luciferase, Luc2.

Funding

This work was supported by the Fundação de Amparo à Pesquisa do Estado de São Paulo [grant number 2015/09,080–2], Brazil. This study was financed in part by the Coordenação de Aperfeiçoamento de Pessoal de Nível Superior - Brasil (CAPES) - Finance Code 001. SRBU is the recipient of a senior researcher scholarship from CNPq. VSA and CT were fellows supported by FAPESP (2015/26,121–4 and 2015/23,832–7, respectively).

Declaration of Competing Interest

The authors declare that they have no known competing financial interests or personal relationships that could have appeared to influence the work reported in this paper.

Acknowledgements

We would like to thank Caroline R. Espada, Jenicer K. U. Yokoyama-Yasunaka and Marinete Pedro da Silva for all the support, technical assistance and constructive discussions.

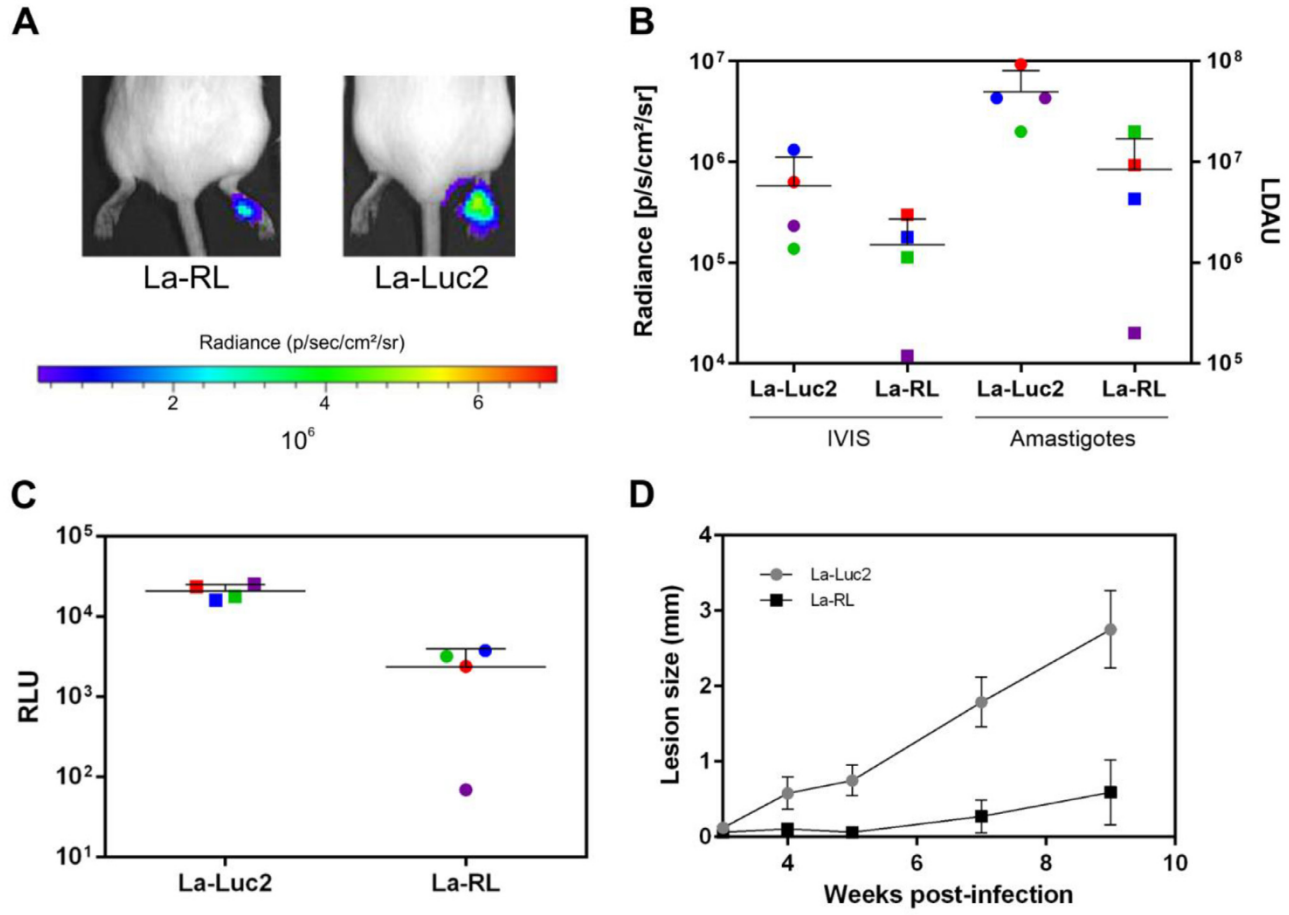

Fig. 5. ***In vivo*** **and** ***ex vivo*** **comparison of light emission between La-RL and La-Luc2.** BALB/c mice (n = 4) were inoculated with 10^6 La-RL or La-Luc2 promastigotes at the left hind footpad. Parasite burden was determined after 9 weeks of infection by bioimaging (**A** and **B**), limiting dilution **(B)** and *ex vivo* bioluminescence activity of amastigotes **(C)**. Colours represent the same animal over different experiments. **(D)** Follow up of the lesion size. Data are the average and standard deviation of the biological replicates.

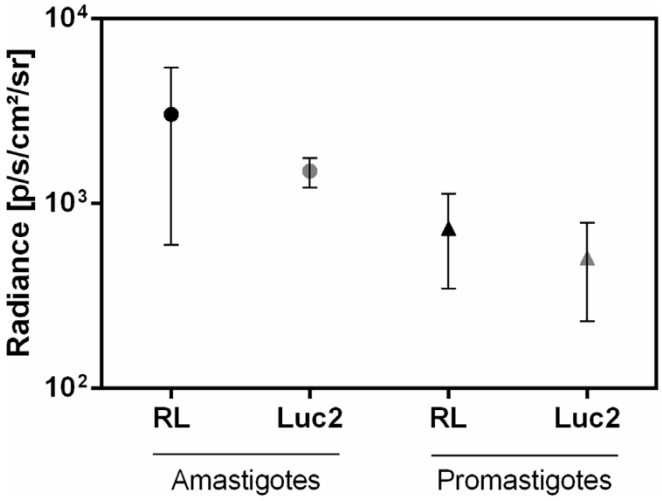

Fig. 6. ***In vivo*** **bioluminescence of 10^5 promastigotes or amastigotes of La-RL and La-Luc2.** BALB/c mice (n = 2) were inoculated in the footpad with 10^5 promastigotes or amastigotes. Bioluminescence was evaluated 1-hour post-inoculation. Data are the average and standard deviation of the biological replicates. RLU: relative light units.

Supplementary materials

Supplementary material associated with this article can be found, in the online version, at doi:10.1016/j.actatropica.2020.105444.

References

Akhoundi, M., Kuhls, K., Cannet, A., Votýpka, J., Marty, P., Delaunay, P., Sereno, D., 2016. A Historical overview of the classification, evolution, and dispersion of *Leishmania* parasites and sandflies. PLoS Negl. Trop. Dis. 10, 1–40. https://doi.org/10.1371/journal.pntd.0004349.

Álvarez-Velilla, R., Gutiérrez-Corbo, M., del, C., Punzón, C., Pérez-Pertejo, M.Y., Balaña-Fouce, R., Fresno, M., Reguera, R.M., 2019. A chronic bioluminescent model of experimental visceral leishmaniasis for accelerating drug discovery. PLoS Negl. Trop. Dis. 13, 1–15. https://doi.org/10.1371/journal.pntd.0007133.

Avci, P., Karimi, M., Sadasivam, M., Antunes-Melo, W.C., Carrasco, E., Hamblin, M.R., 2018. In-vivo monitoring of infectious diseases in living animals using bioluminescence imaging. Virulence 9, 28–63. https://doi.org/10.1080/21505594.2017.1371897.

Bern, C., Desjeux, P., Cano, J., Alvar, J., 2012. Leishmaniasis worldwide and global estimates of its incidence 7. 10.1371/journal.pone.0035671.

Berry, S.L., Hameed, H., Thomason, A., Maciej-Hulme, M.L., Saif Abou-Akkada, S., Horrocks, P., Price, H.P., 2018. Development of NanoLuc-PEST expressing *Leishmania mexicana* as a new drug discovery tool for axenic- and intramacrophage-based assays. PLoS Negl. Trop. Dis. 12, 1–20. https://doi.org/10.1371/journal.pntd.0006639.

Branchini, B.R., Ablamsky, D.M., Davis, A.L., Southworth, T.L., Butler, B., Fan, F., Jathoul, A.P., Pule, M.A., 2010. Red-emitting luciferases for bioluminescence reporter and imaging applications. Anal. Biochem. 396, 290–297. https://doi.org/10.1016/j.ab.2009.09.009.

Branchini, Bruce R., Southworth, T.L., Khattak, N.F., Michelini, E., Roda, A., 2005a. Red- and green-emitting firefly luciferase mutants for bioluminescent reporter applications. Anal. Biochem. 345, 140–148. https://doi.org/10.1016/j.ab.2005.07.015.

Branchini, Bruce R, Southworth, T.L., Murtiashaw, M.H., Wilkinson, S.R., Khattak, N.F.,

Rosenberg, J.C., Zimmer, M., 2005b. Mutagenesis evidence that the partial reactions of firefly bioluminescence are catalyzed by different conformations of the luciferase C-terminal domain. Biochemistry 44, 1385–1393. https://doi.org/10.1021/bi047903f.

Brooks, D.R., Denise, H., Westrop, G.D., Coombs, G.H., Mottram, J.C., 2001. The stage-regulated expression of *Leishmania mexicana* CPB cysteine proteases is mediated by an intercistronic sequence element. J. Biol. Chem. 276, 47061–47069. https://doi.org/10.1074/jbc.M108498200.

Burza, S., Croft, S.L., Boelaert, M., 2018. Leishmaniasis. Lancet. https://doi.org/10.1016/S0140-6736(18)31204-2.

Calvo-Alvarez, E., Cren-Travaillé, C., Crouzols, A., Rotureau, B., 2018. A new chimeric triple reporter fusion protein as a tool for *in vitro* and *in vivo* multimodal imaging to monitor the development of African trypanosomes and *Leishmania* parasites. Infect. Genet. Evol. https://doi.org/10.1016/j.meegid.2018.01.011.

Calvo-Álvarez, E., Stamatakis, K., Punzón, C., Álvarez-Velilla, R., Tejería, A., Escudero-Martínez, J.M., Pérez-Pertejo, Y., Fresno, M., Balaña-Fouce, R., Reguera, R.M., 2015. Infrared fluorescent imaging as a potent tool for *in vitro, ex vivo* and *in vivo* models of visceral leishmaniasis. PLoS Negl. Trop. Dis. 9, 1–19. https://doi.org/10.1371/journal.pntd.0003666.

Coburn, C.M., Otteman, K.M., McNeely, T., Turco, S.J., Beverley, S.M., 1991. Stable DNA transfection of a wide range of trypanosomatids. Mol. Biochem. Parasitol. 46, 169–179. https://doi.org/10.1016/0166-6851(91)90210-W.

Coelho, A.C., Trinconi, C.T., Costa, C.H.N., Uliana, S.R.B., 2014. *In vitro* and *in vivo* miltefosine susceptibility of a *Leishmania amazonensis* isolate from a patient with diffuse cutaneous leishmaniasis. PLoS Negl. Trop. Dis. 8, 1–11. https://doi.org/10.1371/journal.pntd.0002999.

Convit, J., Fernandez, C., Tapia, F., Caceres-Dittmar, G., Castés, M., Rondon, A., Ulrich, M., 1993. The clinical and immunological spectrum of American cutaneous leishmaniasis. Trans. R. Soc. Trop. Med. Hyg. 87, 444–448.

De Niz, M., Spadin, F., Marti, M., Stein, J.V., Frenz, M., Frischknecht, F., 2019. Toolbox for *in vivo* imaging of host–parasite interactions at multiple scales. Trends Parasitol. 35, 193–212. https://doi.org/10.1016/j.pt.2019.01.002.

Eberhardt, E., Bulté, D., Van Bockstal, L., Van Den Kerkhof, M., Cos, P., Delputte, P., Hendrickx, S., Maes, L., Caljon, G., 2019. Miltefosine enhances the fitness of a non-virulent drug-resistant *Leishmania infantum* strain. J. Antimicrob. Chemother. 74, 395–406. https://doi.org/10.1093/jac/dky450.

García-Alai, M.M., Gallo, M., Salame, M., Wetzler, D.E., McBride, A.A., Paci, M., Cicero, D.O., de Prat-Gay, G., 2006. Molecular basis for phosphorylation-dependent, PEST-mediated protein turnover. Structure 14, 309–319. https://doi.org/10.1016/j.str.2005.11.012.

Hall, M.P., Unch, J., Binkowski, B.F., Valley, M.P., Butler, B.L., Wood, M.G., Otto, P., Zimmerman, K., Vidugiris, G., MacHleidt, T., Robers, M.B., Benink, H.A., Eggers, C.T., Slater, M.R., Meisenheimer, P.L., Klaubert, D.H., Fan, F., Encell, L.P., Wood, K.V., 2012. Engineered luciferase reporter from a deep sea shrimp utilizing a novel imidazopyrazinone substrate. ACS Chem. Biol. 7, 1848–1857. https://doi.org/10.1021/cb3002478.

Iwano, S., Sugiyama, M., Hama, H., Watakabe, A., Hasegawa, N., Kuchimaru, T., Tanaka, K.Z., Takahashi, M., Ishida, Y., Hata, J., Shimozono, S., Namiki, K., Fukano, T., Kiyama, M., Okano, H., Kizaka-kondoh, S., Mchugh, T.J., Yamamori, T., Hioki, H., Maki, S., Miyawaki, A., 2018. Single-cell bioluminescence imaging of deep tissue in freely moving animals. Science (80-.) 939, 935–939.

Jaiswal, A.K., Rao, K.B., Kushwaha, P., Rawat, K., Modukuri, R.K., Khare, P., Joshi, S., Mishra, S., Rai, A., Sashidhara, K.V., Dube, A., 2016. Development of *Leishmania donovani* stably expressing DsRed for flow cytometry-based drug screening using chalcone thiazolyl-hydrazone as a new antileishmanial target. Int. J. Antimicrob. Agents. https://doi.org/10.1016/j.ijantimicag.2016.09.018.

Kuchimaru, T., Iwano, S., Kiyama, M., Mitsumata, S., Kadonosono, T., Niwa, H., Maki, S., Kizaka-Kondoh, S., 2016. A luciferin analogue generating near-infrared bioluminescence achieves highly sensitive deep-tissue imaging. Nat. Commun. 7, 1–8. https://doi.org/10.1038/ncomms11856.

Lima, H.C., Bleyenberg, J.A., Titus, R.G., 1997. A simple method for quantifying *Leishmania* in tissues of infected animals. Parasitol. Today 13, 80–82. https://doi.org/10.1016/S0169-4758(96)40010-2.

Magalhães, R.D.M., Duarte, M.C., Mattos, E.C., Martins, V.T., Lage, P.S., Chávez-Fumagalli, M.A., Lage, D.P., Menezes-Souza, D., Régis, W.C.B., Manso Alves, M.J., Soto, M., Tavares, C.A.P., Nagen, R.A.P., Coelho, E.A.F., 2014. Identification of differentially expressed proteins from *Leishmania amazonensis* associated with the loss of virulence of the parasites. PLoS Negl. Trop. Dis. 8. https://doi.org/10.1371/journal.pntd.0002764.

Mißlitz, A., Mottram, J.C., Overath, P., Aebischer, T., 2000. Targeted integration into a rRNA locus results in uniform and high level expression of transgenes in *Leishmania* amastigotes. Mol. Biochem. Parasitol. 107, 251–261. https://doi.org/10.1016/S0166-6851(00)00195-X.

Ponte-Sucre, A., Gamarro, F., Dujardin, J.-.C., Barrett, M.P., López-Vélez, R., García-Hernández, R., Pountain, A.W., Mwenechanya, R., Papadopoulou, B., 2017. Drug resistance and treatment failure in leishmaniasis: a 21st century challenge. PLoS Negl. Trop. Dis. 11, e0006052. https://doi.org/10.1371/journal.pntd.0006052.

Rechsteiner, M., Rogers, S.W., 1996. PEST sequences and regulation by proteolysis. Trends Biochem. Sci. 21, 267–271. https://doi.org/10.1016/0968-0004(96)10031-1.

Reimão, J.Q., Oliveira, J.C., Trinconi, C.T., Cotrim, P.C., Coelho, A.C., Uliana, S.R.B., 2015. Generation of luciferase-expressing *Leishmania infantum chagasi* and assessment of miltefosine efficacy in infected hamsters through bioimaging. PLoS Negl. Trop. Dis. 9, e0003556. https://doi.org/10.1371/journal.pntd.0003556.

Reimão, J.Q., Trinconi, C.T., Yokoyama-Yasunaka, J.K., Miguel, D.C., Kalil, S.P., Uliana, S.R.B., 2013. Parasite burden in *Leishmania (Leishmania) amazonensis* -infected mice: validation of luciferase as a quantitative tool. J. Microbiol. Methods 93, 95–101. https://doi.org/10.1016/j.mimet.2013.02.007.

Rocha, M.N., Corrêa, C.M., Melo, M.N., Beverley, S.M., Martins-Filho, O.A., Madureira, A.P., Soares, R.P., 2013. An alternative *in vitro* drug screening test using *Leishmania amazonensis* transfected with red fluorescent protein. Diagn. Microbiol. Infect. Dis. https://doi.org/10.1016/j.diagmicrobio.2012.11.018.

Sundar, S., Olliaro, P.L., 2007. Miltefosine in the treatment of leishmaniasis: clinical evidence for informed clinical risk management. Ther. Clin. Risk Manag. 3, 733–740.

Sundar, S., Singh, A., 2018. Chemotherapeutics of Visceral Leishmaniasis: present and future developments. Parasitology 145, 481–489. https://doi.org/10.1016/j.physbeh.2017.03.040.

Thorne, N., Inglese, J., Auld, D.S., 2010. Illuminating insights into firefly luciferase and other bioluminescent reporters used in chemical biology. Chem. Biol. 17, 646–657. https://doi.org/10.1016/j.chembiol.2010.05.012.

Trinconi, C.T., Reimão, J.Q., Bonano, V.I., Espada, C.R., Miguel, D.C., Yokoyama-Yasunaka, J.K.U., Uliana, S.R.B., 2018. Topical tamoxifen in the therapy of cutaneous leishmaniasis. Parasitology 1–7. https://doi.org/10.1017/S0031182017000130.

Trinconi, C.T., Reimão, J.Q., Coelho, A.C., Uliana, S.R.B., 2016. Efficacy of tamoxifen and miltefosine combined therapy for cutaneous leishmaniasis in the murine model of infection with *Leishmania amazonensis*. J. Antimicrob. Chemother. 71, 1314–1322. https://doi.org/10.1093/jac/dkv495.

Uliana, S.R.B., Affonso, M.H.T., Camargo, E.P., Floeter-Winter, L.M., 1991. *Leishmania*: genus identification based on a specific sequence of the 18S ribosomal RNA sequence. Exp. Parasitol. 72, 157–163. https://doi.org/10.1016/0014-4894(91)90133-H.

Uliana, S.R.B., Goyal, N., Freymüller, E., Smith, D.F., 1999. *Leishmania*: overexpression and comparative structural analysis of the stage-regulated meta 1 gene. Exp. Parasitol. 92, 183–191. https://doi.org/10.1006/expr.1999.4410.

Uliana, S.R.B., Trinconi, C.T., Coelho, A.C., 2017. Chemotherapy of leishmaniasis: present challenges. Parasitology 1–17. https://doi.org/10.1017/S0031182016002523.

Yan, Y., Shi, P., Song, W., Bi, S., 2019. Chemiluminescence and bioluminescence imaging for biosensing and therapy: *in vitro* and *in vivo* perspectives. Theranostics 9, 4047–4065. https://doi.org/10.7150/thno.33228.

Yeh, H.-.W., Karmach, O., Ji, A., Carter, D., Martins-Green, M.M., Ai, H., 2017. Red-shifted luciferase–luciferin pairs for enhanced bioluminescence imaging. Nat. Methods 14, 971–974. https://doi.org/10.1038/nmeth.4400.

Zerpa, O., Ulrich, M., Blanco, B., Polegre, M., Avila, A., Matos, N., Mendoza, I., Pratlong, F., Ravel, C., Convit, J., 2007. Diffuse cutaneous leishmaniasis responds to miltefosine but then relapses. Br. J. Dermatol. 156, 1328–1335. https://doi.org/10.1111/j.1365-2133.2007.07872.x.